Characterization of *Caenorhabditis elegans* Exonuclease-3 and Evidence That a Mg^{2+}-Dependent Variant Exhibits a Distinct Mode of Action on Damaged DNA†

Andrea Shatilla,‡ Alexander A. Ishchenko,§ Murat Saparbaev,§ and Dindial Ramotar*,‡

University of Montreal, Maisonneuve-Rosemont Hospital, Guy-Bernier Research Centre, 5415 de l'Assomption, Montreal, Quebec, Canada, H1T 2M4, and Groupe "Réparation de l'ADN", UMR 8126 CNRS, Institut Gustave Roussy, 94805 Villejuif Cedex, France

Received February 2, 2005; Revised Manuscript Received July 25, 2005

ABSTRACT: The *Caenorhabditis elegans* genes, *exo-3* and *apn-1*, encode the proteins EXO-3 and APN-1, belonging to the exo III and endo IV families of apurinic/apyrimidinic (AP) endonucleases/3′-diesterases, respectively. Homologues of EXO-3 and APN-1 in *E. coli* and yeast have been clearly documented to repair AP sites and DNA strand breaks with blocked 3′ ends to prevent genomic instability. Herein, we purified the *C. elegans* EXO-3, expressed as a Gst-fusion protein in yeast, and demonstrated that it possesses strong AP endonuclease and 3′-diesterase activities. However, unlike the *E. coli* counterpart exonuclease III, EXO-3 shows no significant level of 3′ → 5′ exonuclease activity following incision at AP sites. In addition, EXO-3 lacks the ability to directly incise DNA at the 5′ side of various oxidatively damaged bases, as observed for the human counterpart Ape1, suggesting that *C. elegans* evolved a member with tailored functions. Importantly, a variant form of EXO-3, E68A, demonstrates altered magnesium-binding properties, and although the *in vitro* AP endonuclease is nearly fully recovered in the presence of $MgCl_2$, the 3′-diesterase activity is reduced when compared to the native enzyme. We suggest that Glu68 plays a role in coordinating Mg^{2+} binding for the enzyme catalytic mechanism. Further analysis reveals that neither purified Gst-EXO-3 nor the E68A variant forms a readily detectable DNA−protein complex with an oligonucleotide substrate containing either an AP site or an α,β-unsaturated aldehyde at its 3′ end. However, if the reaction is conducted in the presence of crude extracts derived from either yeast or *C. elegans* embryos, only E68A forms a distinct slow migrating DNA−protein complex with each of the substrates, suggesting that Glu68 may be required to facilitate the release of EXO-3 from the incised DNA to allow entry of the remaining components of the base-excision repair pathway. Thus, the slow migrating DNA−protein complex formed by the E68A variant could be indicative of a stalled repair process with associated factor(s).

Damage to the DNA base can occur spontaneously or in response to a number of exogenous agents. DNA glycosylases initiate the base-excision repair (BER) pathway by cleaving the *N*-glycosyl bond linking the damaged base to the sugar to form the secondary DNA lesion, the apurinic/apyrimidinic (AP)[1] site (*1*, *2*). Alternatively, DNA can undergo spontaneous depurination or depyrimidination to generate AP sites (*3*). In either case, AP sites are noncoding and can be highly mutagenic or lethal and, therefore, must be removed. AP sites are repaired by hydrolytic AP endonucleases, which are the second enzymes after DNA glycosylases in the BER pathway. These enzymes cleave the phosphodiester bond 5′ to the AP site to generate a 3′-hydroxyl group and a 5′-deoxyribose phosphate (*4*, *5*). In addition to the removal of AP sites, most hydrolytic AP endonucleases also possess a 3′-repair diesterase activity, which removes a variety of 3′-blocking groups, such as the 3′ phosphates and 3′ phosphoglycolates that are present at single-strand breaks generated by oxidative agents, and the 3′-α,β unsaturated aldehydes that are generated at AP sites by AP lyases (*4*, *5*). These enzymes also have the ability to remove one or more nucleotides from the nicked AP sites by the action of a 3′ → 5′ exonuclease activity (*6*−*8*). However, the strength of this latter activity varies among the enzymes and strongly depends upon the reaction conditions (*7*, *9*, *10*).

There are two distinct families of hydrolytic AP endonucleases, exemplified by *Escherichia coli* exonuclease III (exo III) and endonuclease IV (endo IV) (*5*, *11*). In *E. coli*, exo III is expressed constitutively and comprises about 90% of

† This work was funded by the Natural Sciences and Engineering Research Council of Canada to D.R. and by the Association pour la Recherche sur le Cancer and Electricité de France Contrat Radioprotection to M.S. D.R. is supported by a senior fellowship from the Fonds de la Recherche en Sante du Quebec.

* To whom correspondence should be addressed: University of Montreal, Maisonneuve-Rosemont Hospital, Guy-Bernier Research Centre, 5415 de l'Assomption, Montreal, Quebec, Canada, H1T 2M4. Telephone: (514) 252-3400 ext. 4684. Fax: (514) 252-3430. E-mail: dramotar.hmr@ssss.gouv.qc.ca.

‡ University of Montreal, Maisonneuve-Rosemont Hospital.

§ Groupe "Réparation de l'ADN".

[1] Abbreviations: AP, apurinic/apyrimidinic; endo IV, endonuclease IV; exo III, exonuclease III; endo III, endonuclease III; MMS, methyl methane sulfonate; H_2O_2, hydrogen peroxide; DTT, dithiothreitol; Ung, uracil DNA glycosylase; Ugi, uracil glycosylase inhibitor; dHU, 5,6-dihydrouracil; THF, tetrahydrofuran; αdA, α-anomeric 2′-deoxyadenosine; C1 and C2, complexes 1 and 2; C3 and C4, nonrelevant complexes C3 and C4.

10.1021/bi050195t CCC: $30.25
Published on Web 09/01/2005

Table 1: Primers Used in This Study

primer name	sequence (5′ → 3′)	corresponds to
Gst-1	GGGCTGGCAAGCCACGTTTGGTG	Gst-1 in pYEX-Phiz nucleotides 51−74 upstream of MCS
CeExo-4	TTCGACACTGCCGGACGTCT	nucleotides 381−400 of exo-3
CeExo-6	AATCAAATCGAAATAAAACC	nucleotides 601−620 of exo-3
CeExo3-YEX-F1	TTCGATGATGAAGATACCCCACCAAACCCAAAAAAAG AGATCGAA atg tcg aag cga aaa gca gaa gaa gc	plasmid pTW340 and nucleotides 18−43 of exo-3
CeExo3-YEX-R1	TTCAGTATCTACGATTCATAGATCTCTGCAGGTCGACG GATCCCC tta gaa gtc gat ttg cat gac g	plasmid pTW340 and nucleotides 884−863 of exo-3
E68A-FW	CGTTTTTCTAGGAG**C**GACCAAGTGTAAGGAGTGG	nucleotides 206−239 of exo-3
E68A-DW	CCACTCCTTACACTTGGTC**G**CTCCTAGAAAAACG	complementary to E68A-FW
D190A-FW	GTTGCACATAATGAAATTG**C**TCTGAAAAATCCAG	nucleotides 567−600 of exo-3
D190A-DW	CTGGATTTTTCAGA**G**CAATTTCATTATGTGCAAC	complementary to D190A-FW

the AP endonuclease and 3′-diesterase activities, whereas endo IV comprises only 10% of these activities in the uninduced cell but can be induced up to 20-fold by oxidants such as paraquat (*12*). Both families are conserved in the yeast *Saccharomyces cerevisae*, but in this case, Apn1, the endo IV homologue, comprises the major constitutive activity, whereas Apn2, the exo III family member, comprises a minor inducible activity (*13*−*16*). In mammals, only members of the exo III family have been identified, and in humans, Ape1 and Ape2 comprise two distinct subclasses of this family (*17*, *18*).

Unlike other multicellular eukaryotes, *Caenorhabditis elegans* possesses members from both families of AP endonucleases, EXO-3 (homologous to *Escherichia coli* exo III) and APN-1 (homologous to *E. coli* endo IV) (accession number AF034258) (*19*). Expression of either *C. elegans* EXO-3 or APN-1 rescues the DNA-repair defects, as well as suppresses the high spontaneous mutation frequency, of a yeast mutant lacking both Apn1 and Apn2 (*20*). In this study, we purify one of the enzymes EXO-3 as a Gst-fusion protein (Gst-EXO-3) and demonstrate that it possesses strong AP endonuclease and 3′-phosphodiesterase activities, as well as a 3′ → 5′ exonuclease activity that is detectable under specialized buffer conditions. Our data revealed that *C. elegans* EXO-3 displays features different from *E. coli* exonuclease III and human Ape1. Consistent with this notion, we show that a variant form of Gst-EXO-3, Gst-E68A, binds less tightly to Mg^{2+} but exhibits a significant level of AP endonuclease and a reduced 3′-repair diesterase activity, only in the presence of Mg^{2+}. This contrasts the observation reported for the corresponding E96A hApe1 mutant, which has dramatically reduced enzymatic activities under the same conditions (*21*, *22*). Thus, it would appear that Glu68 of EXO-3 plays a role in coordinating Mg^{2+} for the enzyme mechanistic functions. We further show that the variant Gst-E68A but not the native Gst-EXO-3 forms a distinct slow migrating DNA−protein complex with either an AP site or a 3′-α,β unsaturated aldehyde substrate in the presence of crude extracts derived from either yeast or *C. elegans* embryos. While this latter observation has many implications, it suggests that Glu68 of EXO-3 may serve to facilitate the release of the enzyme from the incised AP-site lesions, thereby allowing completion of the repair process by components of the base-excision repair pathway.

MATERIALS AND METHODS

Yeast and Bacterial Strains. Saccharomyces cerevisiae laboratory strains YW465 (*MAT*α *ade2*Δ*0 his3*Δ*-200 leu2*Δ*-1 met15*Δ*0 trp1*Δ*-63 ura3*Δ*0*), which is wild-type for AP endonuclease, 3′-diesterase, and 3′- phosphatase activities, its isogenic triple mutant derivative YW778 (*apn1*Δ*::HIS3 apn2*Δ*::KanMX4* tpp1Δ*::MET15*) and YW607 (*MAT*α *his3D200 leu2*−*3,112 pep4::HIS3 ura3*−*52*) were generously provided by Dr. Tom Wilson (Ann Arbor, MI). Strain YW607 was maintained on YPD agar, and strains YW465 and YW778 were maintained on YPD agar supplemented with adenine (20 μg/mL). *E. coli* laboratory strain DH5α (used for amplification of plasmids) was maintained on Luria Broth (LB) agar.

Proteins. Purifications of the endo IV and Apn1 protein were performed as described (*23*, *24*). Endo III and Ugi were generously provided by Dr. Bob Melamede, University of Vermont, VT, and the late Dr. Dale Mosbaugh, Oregon State University, OR, respectively.

Construction of the GST-Fusion Protein. The plasmid pTW340 (provided by Dr. Tom Wilson, Ann Arbor, MI) contains the Ogg1 gene fused to GST, under the control of the copper-inducible promoter P_{CUP1} in the dual host expression vector pYEX-Phiz (Dr. Eric Phizicky via Dr. Tom Wilson). The vector bears markers for uracil (*URA3*), leucine (*leu2-d*), and ampicillin. The Ogg1 gene was removed by restriction digest using *Eco*R1 and *Sma*1, and the digestion product was electrophoresed on a 1% agarose gel. The fragment corresponding to the linearized vector was excised and purified.

Plasmid pPC86 (Invitrogen) bearing the entire coding sequence of the exo-3 gene (*20*) was used as a template for amplification by PCR using Pfu polymerase (Stratagene, La Jolla, CA) and the primers CeExo3-YEX-F1 and CeExo3-YEX-R1 (Table 1). The PCR product was electrophoresed on a 1% agarose gel, and the fragment corresponding to the desired product was excised and purified as above. To generate the fusion by GAP repair, 100 ng of the linearized vector and 0 or 300−1800 ng of the exo-3 PCR product were co-transformed into *S. cerevisiae* strain YW607. Transformants were selected for on −URA minimal media agar plates.

Extraction of Plasmid DNA from Yeast and Amplification. Cells were resuspended in lysis solution A (10 mM Tris at pH 8.0, 100 mM NaCl, 1 mM EDTA, 2% Triton X-100, and 1% SDS) and then vortexed with 425−600 μm glass beads (Sigma Chemical Co., St. Louis, MO) in the presence of 20% phenol and 20% chloroform, followed by incubation with RNAse A, ethanol precipitation, and resuspension in H_2O. For amplification, the extracted plasmid was transformed into $CaCl_2$-treated *E. coli* strain DH5α as described

by Sambrook et al. (*25*), and transformants were selected for on LB Petri plates containing ampicillin. Plasmids were extracted from *E. coli* as described by Sambrook et al. (*25*).

Expression of the Gst-Fusion Protein in Mutant Yeast. Strain YW778 was transformed with the Gst-exo-3 fusion plasmid extracted from *E. coli*. Transformants were selected for on −URA minimal medium agar plates and grown in −URA −LEU liquid minimal medium for plasmid amplification.

Sequencing of Plasmid DNA. Plasmid DNA isolated from *E. coli* was purified using Concert Rapid Gel Extraction System (Invitrogen, Carlsbad, CA) or Quiaprep spin columns and reagents (Qiagen, Mississauga, Ontario, Canada) and sequenced in an automatic sequencer using the primers Gst-1, CeExo-4, and CeExo-6 (Table 1).

Site-Directed Mutagenesis. Single amino acid substitutions of the Gst-EXO-3 fusion protein in the dual host expression vector pYEX-Phiz (above) bearing markers for ampicillin and uracil were generated using the QuikChange site-directed mutagenesis kit (Stratagene, La Jolla, CA). Briefly, for each mutation, the Gst-exo-3 fusion plasmid was PCR-amplified using two complementary polyacrylamide gel-purified oligonucleotide primers (Table 1) containing the desired mutation. Mutant E68A was generated with the primers E68A-FW and E68A-DW to replace the glutamic acid at position 68 with alanine, and mutant D190A was generated with the primers D190A-FW and D190A-DW to replace the aspartic acid at position 190 with alanine (*20*). The PCR products were treated with Dpn1 to degrade the methylated nonmutated parental DNA templates and then transformed into *E. coli* DH5α for amplification. After sequencing, plasmids containing the desired mutations were transformed into the *S. cerevisiae* triple mutant YW778 and selected for on minimal media agar plates lacking uracil.

Extraction of Proteins. Yeast cells were harvested from liquid culture and washed once with H_2O, and pellets were frozen at −80 °C until needed. For routine and preliminary extractions, cells were resuspended in extraction buffer B (50 mM Tris-HCl at pH 7.4, 30 mM KCl, 10% glycerol (v/v), 1 μg/mL leupeptin, 1 μg/mL aprotinin, 1 mM benzamidine, and 1 mM PMSF) and transferred to 600-μL Eppendorf tubes containing 300 μL of glass beads (425−600 μm), where proteins were extracted using a minibead beater (BioSpec Products, Bartlesville, OK) at 5000 rpm for 20 s (5 cycles). Cellular debris was partially removed by centrifugation in a tabletop microcentrifuge (Jouan, Inc., Winchester, VA) at 9000*g* for 10 min at 4 °C. Proteins were quantified according to the method of Bradford using Bio-Rad Protein Assay Dye Reagent (Bio-Rad Laboratories) and BSA as the standard protein (*26*).

Purification of GST-Fusion Proteins. For purification of Gst-fusion proteins, cells were resuspended in extraction buffer C (50 mM Tris-HCl at pH 7.5, 4 mM $MgCl_2$, 1 mM EDTA, 5 mM DTT, 1 M NaCl, 10% glycerol, 1 μg/mL leupeptin, 1 μg/mL aprotinin, 1 mM benzamidine, and 1 mM PMSF) and transferred to a MAXI beadbeater (BioSpec Products, Bartlesville, OK) containing $^1/_2$ of its volume of 425−600 μm of glass beads, where proteins were extracted for 20 s (12 cycles). Cellular debris was partially removed by centrifugation at 12 000 rpm (SS34 rotor). Gst-EXO-3 fusion protein was affinity-purified using Glutathione Sepharose 4B Beads (Amersham Biosciences Corp, Piscataway, NJ). Binding of the Gst-fusion protein to the beads was carried out by incubation of the crude protein extract with PBS-equilibrated Gst Sepharose Beads in 15-mL falcon tubes with gentle agitation at 4 °C overnight. Unbound proteins and other components of the crude extract were removed from the beads by centrifugation at 1000 rpm (Sorvall RT 7) at 4 °C for 30 s. The beads were washed 3 times with 100 volumes of chilled PBS and transferred to 1.5-mL Eppendorf tubes. The Gst-fusion protein was separated from the beads at room temperature by four incubations (10 min each) with 50 mM Tris and 10 mM reduced glutathione at pH 8.0 (ICN Biomedicals, Inc.). Each time the protein released from the beads was collected by centrifugation in a tabletop microcentrifuge (Sigma 1−15) at 2000 rpm for 30 s. The supernatants were dialyzed twice against 20 mM Tris-HCl at pH 7.5, 4 mM $MgCl_2$, 2 mM EDTA, 55 mM NaCl, and 1 mM DTT in the presence of 20% glycerol (first dialysis) and 50% glycerol (second dialysis) at 4 °C. Purified protein was aliquoted into small portions and stored at −20 °C.

SDS−PAGE and Western Blot. Crude extracts and purified proteins were electrophoresed on two identical 10% acrylamide/bis-acrylamide (29:1) gels containing SDS. The proteins from one gel were transferred to nitrocellulose Hybond C extra (Amersham Biosciences Corp, Piscataway, NJ). The membrane was stained with Ponceau S to verify equal loading and efficiency of transfer. Gst-fusion proteins were detected by immunoblotting overnight with 0.0002% Anti-Glutathione-*S*-Transferase developped in rabbit (Sigma Chemical Co., St. Louis, MO), followed by 4 washes and a 2 h incubation with 0.0002% anti-rabbit Ig, Horseradish Peroxidase linked whole antibody from donkey (Amersham Biosciences Corp, Piscataway, NJ) and revealed by Western Lightning Chemiluminescence (Perkin−Elmer Lifesciences, Woodbridge, Ontario, Canada) using Kodak BioMax Light film (Amersham Biosciences). The proteins from the other gel were silver-stained.

Gradient Plate Assay. Yeast cultures were grown overnight in liquid minimal medium in the absence of uracil. The OD_{600} of each culture was adjusted to 2.0 before being replicated on gradient plates as previously described (*27*). Strains that grew all along the gradient (85 mm) were considered to show 100% growth. In general, this type of gradient provides a rapid way to assess the DNA-repair capacity of a given cell challenged with a DNA-damaging agent. Pictures were taken after 2 days of incubation at 30 °C.

Preparation of Oligonucleotide Substrates. A synthetic 42-base pair 5′-end [^{32}P]-labeled oligonucleotide with a uracil at position 21 d(GCTGCATGCCTGCAGGTCGA**U**TCTAGAGGATCCCGGGTACCT) and complementary strand containing G opposite to U d(CGACGTACGGACGTCCAGCT**G**AGATCTCCTAGGGCCCATGGA) was prepared as previously described (*28*, *29*). For the AP endonuclease assay, the AP substrate was generated by incubating 32 ng of the labeled oligonucleotide with two units of *E. coli* Ung (New England Biolabs) in buffer D (30 mM Hepes-KOH at pH 7.6, 50 mM NaCl, and 2 mM EDTA) for 30 min at 37 °C, followed by heat inactivation at 65 °C for 10 min. For the 3′-diesterase assay, the 3′-blocked end was generated by incubating 16 ng of the AP substrate with 46 ng of purified endonuclease III (generously provided by Dr. Bob Melamede, University of Vermont, VT) in buffer E (50 mM Hepes-

KOH at pH 7.5, 50 mM KCl, 50 μg/mL BSA, and 2 mM EDTA) for 30 min at 37 °C, followed by heat inactivation at 65 °C for 10 min. The product of the reaction was electophoresed on a 10% polyacrylamide gel and visualized by autoradiography to verify that the substrate had been entirely converted prior to use (*28*). The above substrates were also used as probes in the DNA-binding assays. For the nucleotide incision repair assay, the oligonucleotide (30-mer) containing single αdA, 5,6-dihydrouridine (dHU) or tetrahydrofuran (THF) lesions d(TGACTGCATA**X**GCAT-GTAGACGATGTGCAT) where **X** is αdA, dHU, or THF and complementary strands containing either T or dG opposite **X** were purchased from Eurogentec (Seraing, Belgium). The dHU-containing substrate was labeled on the 3′ end with terminal transferase using [^{32}P]dCTP.

Enzyme Activity Assays. For the AP endonuclease and 3′-diesterase assays, 50 ng of the appropriate substrate (see above) was incubated with 6 μg of crude protein extract at 37 °C for 30 min or with the indicated amount of affinity-purified Gst-fusion protein at 37 °C for 30 min unless otherwise stated in a final volume of 12.5 μL. Reactions were stopped with 5 μL formamide loading buffer (76% formamide, 0.3% bromophenol blue, 0.3% xylene cyanole, and 10 mM EDTA). Samples were heated at 65 °C for 3−5 min to dissociate the labeled oligonucleotide from DNA-binding proteins. AP endonuclease and 3′-diesterase assay reaction products were separated on denaturing 10 and 17%, respectively, polyacrylamide−7 M urea gels and viewed by autoradiography (*28*). The nucleotide incision repair assay was performed as described (*30*).

DNA-Binding Assays. Routine reaction mixtures contained 500 pg of 5′-end [^{32}P]-labeled oligonucleotide substrate (see above) with either a uracil at position 21 (modified base substrate), an AP site at position 21 (abasic substrate), or a 3′-α,β unsaturated aldehyde (3′-blocked end substrate), 10 μg of crude protein extract, and/or 100 ng of purified protein in DNA-binding buffer (final volume 24 μL). The DNA-binding buffer consisted of 20 mM Hepes-KOH at pH 7.9, 12% glycerol, 2 mM EDTA, 2 mM DTT, 150 mM KCl, and 20 ng/μL poly dIdC. Ugi was used as indicated. Reaction mixtures were incubated at 25 °C for 20 min, and protein−DNA complexes were resolved on nondenaturing 6% polyacrylamide/bis-acrylamide (39:1) Tris-glycine at pH 8.3 gels at 4 °C (120 V for 4 h) and viewed by autoradiography or phosphorimaging.

RESULTS

Expression and Functional Analysis of Gst-EXO-3 and Two Variants E68A and D190A in Yeast Cells. To characterize the *C. elegans* EXO-3, we first designed an expression plasmid pGst-exo-3 to produce a Gst-EXO-3 fusion protein in the budding yeast *S. cerevisiae*. This was necessary because *E. coli* expression systems failed to produce an active form of EXO-3 (*19*, *20*). Yeast cells harboring plasmid pGst-EXO-3 produced a polypeptide of 62 kDa, corresponding to the expected size of the fusion protein as detected by Western blot probed with anti-Gst antibodies (Figure 1A, lane 3). Similarly, two variants of EXO-3, E68A and D190A, bearing single amino acid substitutions, were also expressed as 62-kDa polypeptides (Figure 1A, lanes 4 and 5, respectively). No major degradation fragment was observed among these fusion proteins, suggesting that Gst-EXO-3 and the variants are stably expressed in yeast cells.

To assess if the expressed fusion protein Gst-EXO-3 is biologically active, the plasmid pGst-exo-3 was tested for the ability to confer to the DNA-repair-deficient yeast strain YW778 resistance to the alkylating agent methyl methane sulfonate (MMS). This mutant strain lacks the AP endonucleases Apn1 and Apn2 and, therefore, displays hypersensitivity to MMS because of an inability to repair MMS-induced AP sites (*15*, *16*). As shown in Figure 1C, plasmid pGst-exo-3 restored full parental MMS resistance to strain YW778. Similar results were obtained if the cells were challenged with H_2O_2, a chemical oxidant that produces DNA-strand breaks with blocked 3′ termini, which must be processed by a 3′ diesterase (*20*). These data indicate that the Gst-EXO-3 fusion protein is functionally active, because it can act *in vivo* to repair MMS- and H_2O_2-induced DNA lesions. Thus, it is reasonable to assume that the Gst fragment attached to EXO-3 does not impair the enzyme activities. As such, we deemed that the Gst-fusion protein is suitable for characterization of EXO-3. It is noteworthy that neither of the variants E68A nor D190A conferred MMS or H_2O_2 resistance to strain YW778 [Figure 1C and (*20*)], suggesting that these proteins might be inactive and therefore incapable of repairing damaged DNA *in vivo* (see below).

Gst-EXO-3 and E68A but not D190A Actively Process Damaged DNA in Vitro. We next verified if the ability of Gst-EXO-3 to confer drug resistance to strain YW778 is a direct result of the processing of damaged DNA. To do this, crude extracts derived from strain YW778 expressing either Gst-EXO-3, Gst-E68A, or Gst-D190A were monitored for the ability to act on various DNA substrates. The substrates used consist of 42-mer oligonucleotide duplexes, which were labeled with ^{32}P on the 5′ end of the strand carrying a centrally located lesion, either an uracil/guanine (U·G) mismatch, an AP site, or a strand break with a 3′-blocked end (Figure 2A, see the Materials and Methods). As expected, the data revealed that extracts derived from the parent (strain YW465) cleaved the U·G substrate to produce a 20-mer product containing a 3′-hydroxyl group (3′-OH) (Figure 2A, lane 3) because of the sequential action of yeast endogenous uracil-DNA glycosylase (Ung) and the AP endonucleases, Apn1 and Apn2. The 20-mer 3′-OH product was not generated by the extract prepared from strain YW778, which is devoid of AP endonuclease activities (Figure 2A, lane 4). However, extracts from strain YW778 produced a different 20-mer product as a consequence of the action of Ung and the presence of AP lyases such as Ntg1, Ntg2, and Ogg1 (Figure 2A, lane 4) (*31*, *32*). These AP lyases can cleave AP sites, following the action of DNA glycosylases (e.g., Ung), to produce a 20-mer product terminated with a 3′ α,β-unsaturated aldehyde, which migrates slightly slower on a polyacrylamide gel than the 20-mer 3′-OH product generated by AP endonucleases (*33*, *34*).

Extracts derived from strain YW778 carrying pGst-exo-3 cleaved the U·G substrate to generate the 20-mer 3′-OH product (Figure 2A, lane 5), suggesting that EXO-3 can enter and nick AP sites following the action of Ung. In addition, the YW778/pGst-exo-3 extract directly cleaved the AP-site substrate to create a 20-mer 3′-OH product (lane 12), indicating that EXO-3 can recognize and nick AP sites. Moreover, the 20-mer substrate carrying a 3′ α,β-unsaturated

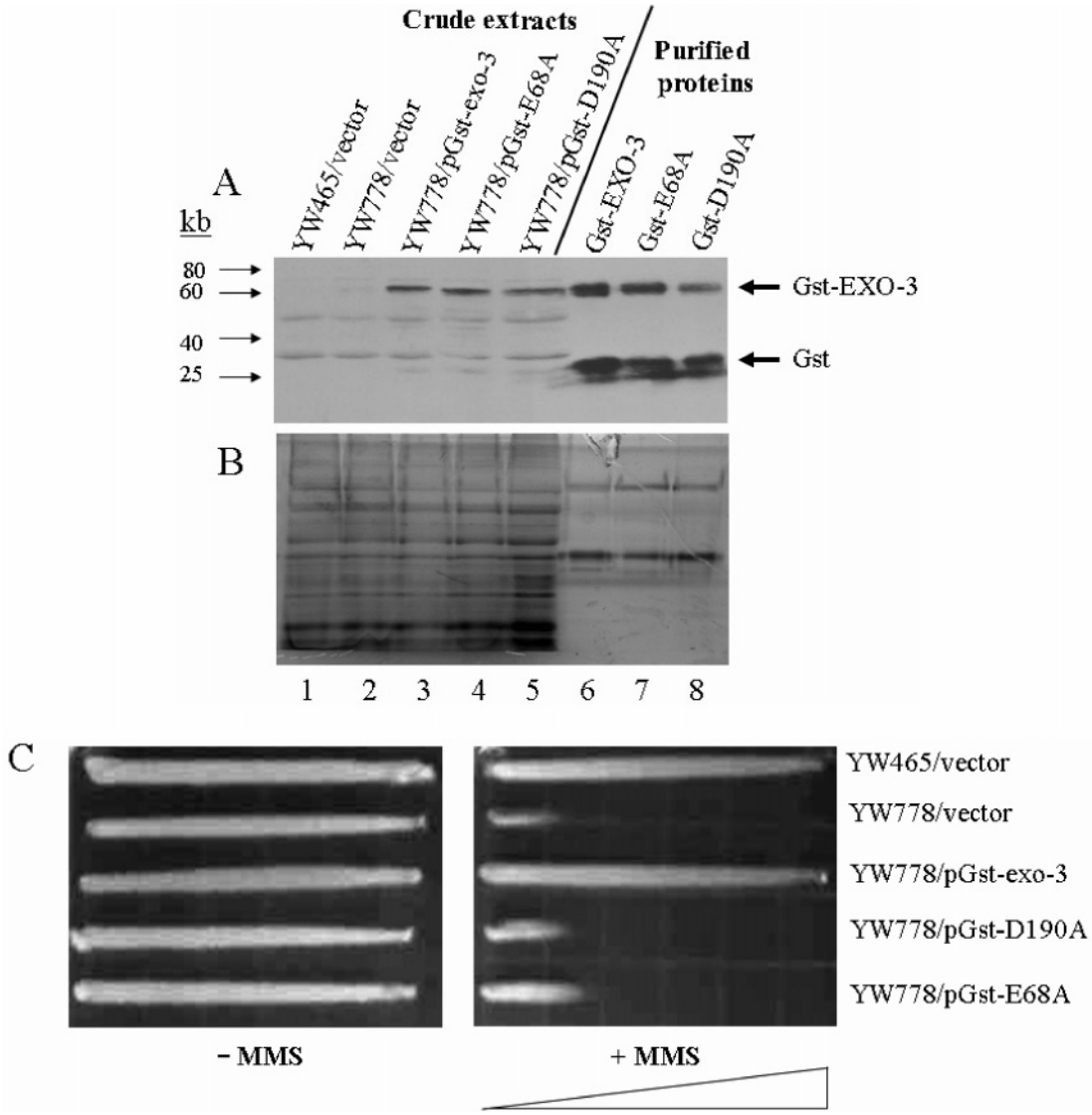

FIGURE 1: Expression and functional analyses of Gst-EXO-3 and the variants E68A and D190A in a yeast DNA-repair-deficient mutant. (A and B) Western blot and silver-stain analyses for expression of Gst-EXO-3 and its variants. Parent (YW465) and the mutant strain (YW778) carrying the indicated vector or plasmid were grown overnight in liquid minimal media, and protein extractions and purifications were carried out as described in the Materials and Methods. Lanes 1−5, 50 μg of crude protein extract; and lanes 6−8, 5 μg of affinity-purified protein. (A) Western blot analysis probed with anti-Gst monoclonal antibodies, and (B) silver-stained gel. Results are representative of at least three independent extractions and purifications. (C) Complementation test for functionality of Gst-EXO-3 and its variants in strain YW778. Parent (YW465) and the mutant strain (YW778) carrying the indicated vector or plasmid were grown overnight in liquid minimal media and replicated onto a solid media gradient without and with methyl methane sulfonate (MMS 0.018 mmol in the bottom layer) (see the Materials and Methods). Growth along the gradient is considered to be 100%. The picture was taken after 2 days of incubation at 30 °C. This assay was repeated at least 3 times with similar results.

aldehyde, prepared by treating the AP-site substrate with the purified AP lyase *E. coli* endonuclease III, was converted to the 20-mer 3′-OH product by the YW778/pGst-exo-3 extract (lane 19), demonstrating that EXO-3 also possesses a 3′-repair diesterase activity. AP endonucleases have previously been shown to contain a 3′-repair diesterase activity that can process the 3′ α,β-unsaturated aldehyde to create a free 3′-OH for DNA-repair synthesis (*35*, *36*). Collectively, the data clearly indicate that EXO-3 possesses the enzymatic properties typically associated with AP endonucleases/3′-repair diesterases such as *E. coli* exonuclease III and endonuclease IV (*37*). Thus, the ability of EXO-3 to confer drug resistance to strain YW778 is a direct result of the protein processing damaged DNA.

Extracts derived from strain YW778 expressing the EXO-3 variants, E68A and D190A, were also assessed for the ability to cleave the AP site and remove the 3′ α,β-unsaturated aldehyde from the DNA substrates. Interestingly, extracts expressing E68A were active at cleaving the AP-site substrate to produce the 20-mer 3′-OH product (Figure 2B, lane 5). In addition, this extract weakly processed the 3′ α,β-unsaturated aldehyde, when compared to the extract expressing the native protein (see below), to produce the 20-mer 3′-OH product (Figure 2C, lane 5 versus 4). Because the E68A variant possesses a significant level of AP endonuclease activity, its inability to confer MMS resistance to strain YW778 (Figure 1C) suggests that it may bear a defect other than incising AP sites *in vivo*. Extracts derived from strain YW778 expressing D190A lacked the ability to cleave either the AP-site substrate (Figure 2B, lane 6) or convert the 3′ α,β-unsaturated aldehyde substrate to the 20-mer 3′-OH product (Figure 2C, lane 6), consistent with the comple-

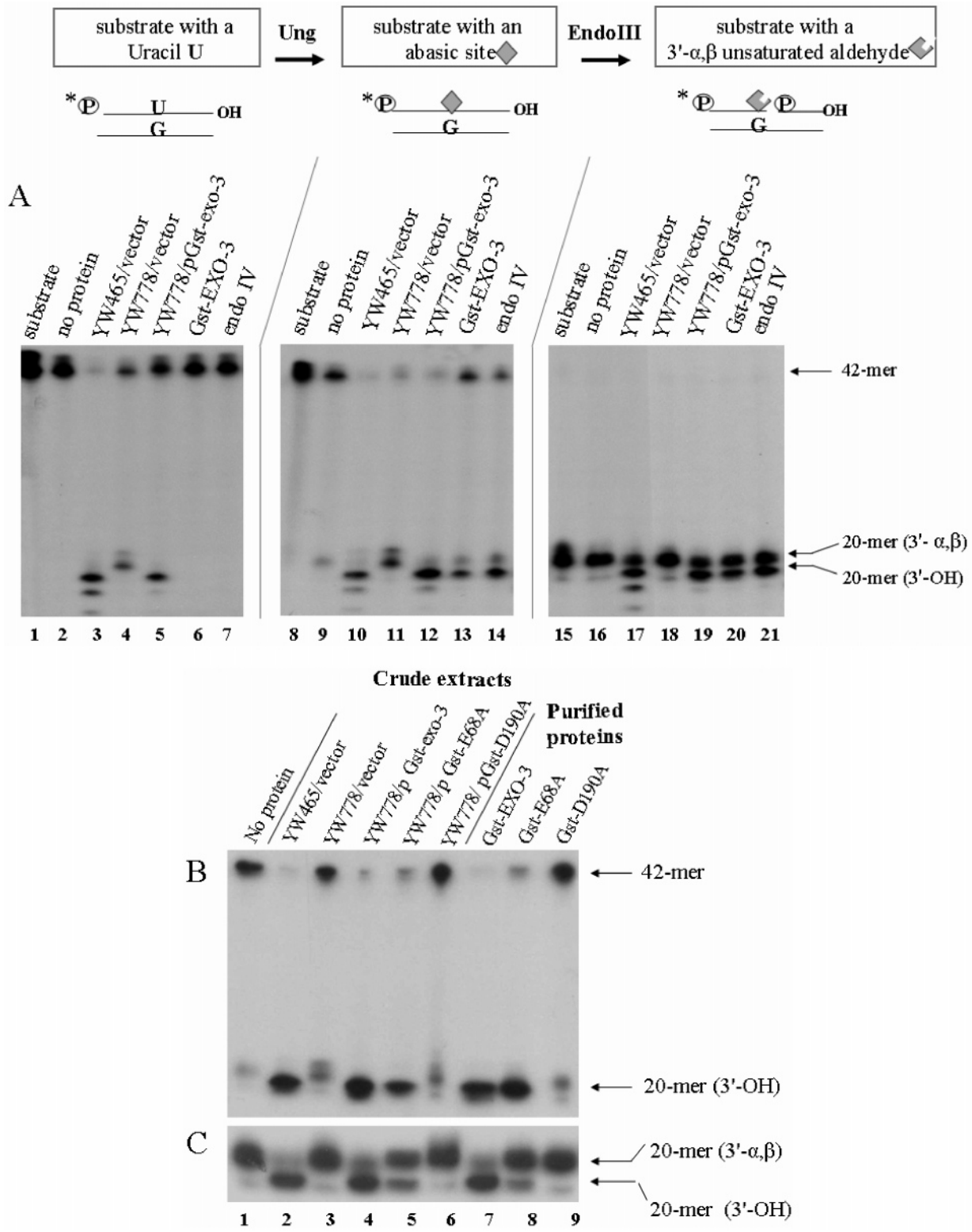

FIGURE 2: *In vitro* analysis for processing of DNA lesions by Gst-EXO-3 and its variants. (A) Either crude extracts prepared from the indicated strains or purified proteins were assayed for the ability to act on a 42-mer double-stranded labeled oligonucleotide substrate containing one of the following single DNA lesions: lanes 1−7, uracil·guanine (U·G) mismatch; lanes 8−14, AP site; and lanes 15−21, DNA strand break with 3′-α,*β* unsaturated aldehyde. Assay reactions carried out in AP buffer (100 mM Tris-HCl at pH 7.0 with 5 mM $MgCl_2$) contained 800 pg of labeled substrate and either 3 *μ*g of crude protein extract derived from the parent (lanes 3, 10, and 17), the mutant strain (lanes 4, 11, 18), the mutant strain expressing Gst-EXO-3 (lanes 5, 12, and 19), 400 ng of affinity-purified Gst-EXO-3 (lanes 6, 13, and 20), or 2 ng of purified *E. coli* endo IV (lanes 7, 14, and 21) in a final volume of 12.5 *μ*L and incubated at 37 °C for 30 min. All assays in A were resolved on a 17% polyacrylamide−7 M urea sequencing gel. (B and C) Processing of AP site and 3′-α,*β* unsaturated aldehyde DNA substrates, respectively. Crude extracts (3 *μ*g) were derived from the parent and the mutant strain carrying the indicated plasmid. The proteins Gst-EXO-3, Gst-E68A, and Gst-D190A were all affinity-purified and used at 400 ng each. Assay conditions were the same as for A, and monitoring for product formation was after resolution on 10% (for the AP-site substrate) and 17% (for the 3′-α,*β* unsaturated aldehyde substrate) polyacrylamide−7 M urea sequencing gels. Arrows indicate positions and sizes of the substrates and reaction products. The results (A−C) are representative of three independent experiments.

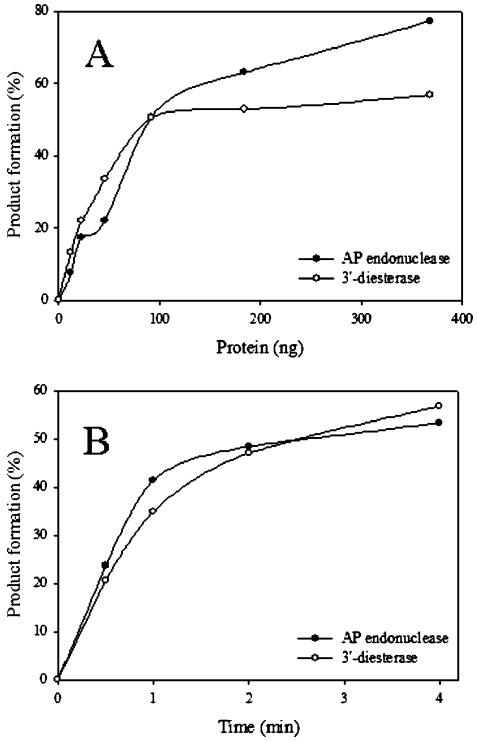

FIGURE 3: Protein concentration- and time-dependent processing of AP site and 3′-α,*β* unsaturated aldehyde by affinity-purified Gst-EXO-3. (A) Product formation by cleavage of the AP site and 3′-α,*β* unsaturated aldehyde substrates with increasing concentrations of purified Gst-EXO-3. Assay conditions were the same as in Figure 2. (B) Time-dependent cleavage of the AP site and 3′-α,*β* unsaturated aldehyde substrate with a fixed concentration of purified Gst-EXO-3. Assay conditions were with 368 ng of purified Gst-EXO-3 at 37 °C for 0−4 min. Product formation was monitored by autoradiography after resolution on 10 and 17% polyacrylamide−7 M urea sequencing gels, and the data were quantified using the Scion Image Beta 4.0.2 computer program. The data are representative of three independent protein purifications.

mentation assay (Figure 1C) that D190A is indeed an inactive protein.

Comparison of the AP Endonuclease and 3′-Repair Diesterase Activity Levels of the Purified Gst-EXO-3. To characterize the DNA-repair functions of EXO-3, we used Gst-EXO-3 affinity purified from strain YW778. Silver-stained gels revealed that the purified Gst-EXO-3 protein contained no major contaminating protein other than a significant level of Gst (Figure 1B, lane 6), as detected by Western blot using anti-Gst antibodies (Figure 1A, lane 6). We have previously observed precise cleavage of the Gst tag from other Gst-fusion proteins in yeast, but the reason for this is unclear (*8*). The purified Gst-EXO-3 was monitored for both AP endonuclease and 3′-diesterase activities over a wide protein concentration range (Figure 3A). The data revealed that conversion of the 42-mer AP substrate to the 20-mer 3′-OH product increased linearly with the protein concentration (Figure 3A). Similarly, conversion of the 3′-α,*β* substrate to the 3′-OH product increased linearly with the protein concentration (Figure 3A). In both cases, ∼50% of the product was produced with 92 ng of purified Gst-EXO-3 (Figure 3A). We also conducted a time-course experiment with the purified Gst-EXO-3 protein to monitor the rate of the reactions. As shown in Figure 3B, the 42-mer AP substrate was converted to the 20-mer 3′-OH product very rapidly, with approximately 50% conversion within 2 min (Figure 3B). Likewise, conversion of the 20-mer 3′-α,*β* substrate to the 20-mer 3′-OH product was also rapid (Figure 3B). These data clearly indicate that the AP endonuclease and 3′-diesterase activities of Gst-EXO-3 are equally active. However, analysis using a higher concentration of proteins revealed that greater than 99% of the AP-site substrate is cleavable, whereas only 61% of the 3′-α,*β* substrate was cleaved. It is noteworthy that during these analyses, we observed that the purified Gst-EXO-3 did not process the 20-mer product to generate a ladder typical of *E. coli* exonuclease III, which has a strong 3′ → 5′ exonuclease activity following cleavage of AP sites (data not shown) (*28*). This observation strongly suggests that the *C. elegans* EXO-3 is different from its *E. coli* counterpart (see below and the Discussion).

Gst-EXO-3 Lacks Nucleotide-Incision Repair Activity. Recent studies demonstrated that hApe1 can make an incision on the 5′ side of oxidized bases in a manner similar to members of the endo IV family (*30*). We tested if purified Gst-EXO-3 could similarly incise a 30-mer double-stranded oligonucleotide carrying either α-deoxyadenosine (α-dA/T) or dihydrouridine (dHU/G) at position 11 on the upper [^{32}P]-labeled strand. The data revealed that, while purified yeast Apn1 cleaved both the α-dA/T and dHU/G substrates to produce the 10- and 21-mer labeled product (Figure 4, lanes 7 and 12, respectively), purified Gst-EXO-3 did not incise these substrates (Figure 4, lanes 8 and 13, respectively). In the control experiment and under the same assay conditions, purified Gst-EXO-3 cleaved the tetrahydrofuran AP site (THF/G) to produce the 10-mer labeled product (Figure 4, lane 3). Thus, it would appear that EXO-3 differs from Apn1, as well as hApe1, by acting on a more restricted range of DNA lesions. Interestingly, under assay conditions optimized for hApe1 cleavage of oxidized bases, the purified Gst-EXO-3 processed the α-dA/T substrate from the 3′ end to generate a ladder typically observed by enzymes with 3′ → 5′ exonuclease activity (Figure 4, lane 9 and 10). This 3′ → 5′ exonuclease activity is associated with Gst-EXO-3 and is not the result of a contaminant, because similar data was obtained with crude extracts derived from strain YW778 carrying plasmid pGst-EXO-3 but not the empty vector (data not shown).

We note that, although thorough kinetic analysis was not performed with the variant E68A on the above substrates, our data revealed that the purified fusion protein possessed a significant level of AP endonuclease activity against both a natural AP site (Figure 2B, lane 8) and THF/G under assay conditions containing $MgCl_2$ (data not shown and see below). However, purified E68A exhibited a weak activity against the 3′-α,*β* unsaturated aldehyde substrate (Figure 2C, lane 8) and, similar to the native Gst-EXO-3, showed no nucleotide-incision repair activities (data not shown). As predicted from the crude extract analysis, the purified variant D190A displayed no detectable AP endonuclease or 3′-diesterase activities (parts B and C of Figure 2, lane 9, respectively).

Purified Gst-EXO-3 Requires Divalent Metal Ions for Enzymatic Activities. Because exo III members are known metal ion-dependent enzymes, we tested the metal ion requirement of the purified Gst-EXO-3. In the absence of exogenous metals, purified Gst-EXO-3 cleaved the AP-site substrate to generate the 20-mer 3′-OH product (Figure 5A, lane 1). However, the activity was attributed to the $MgCl_2$

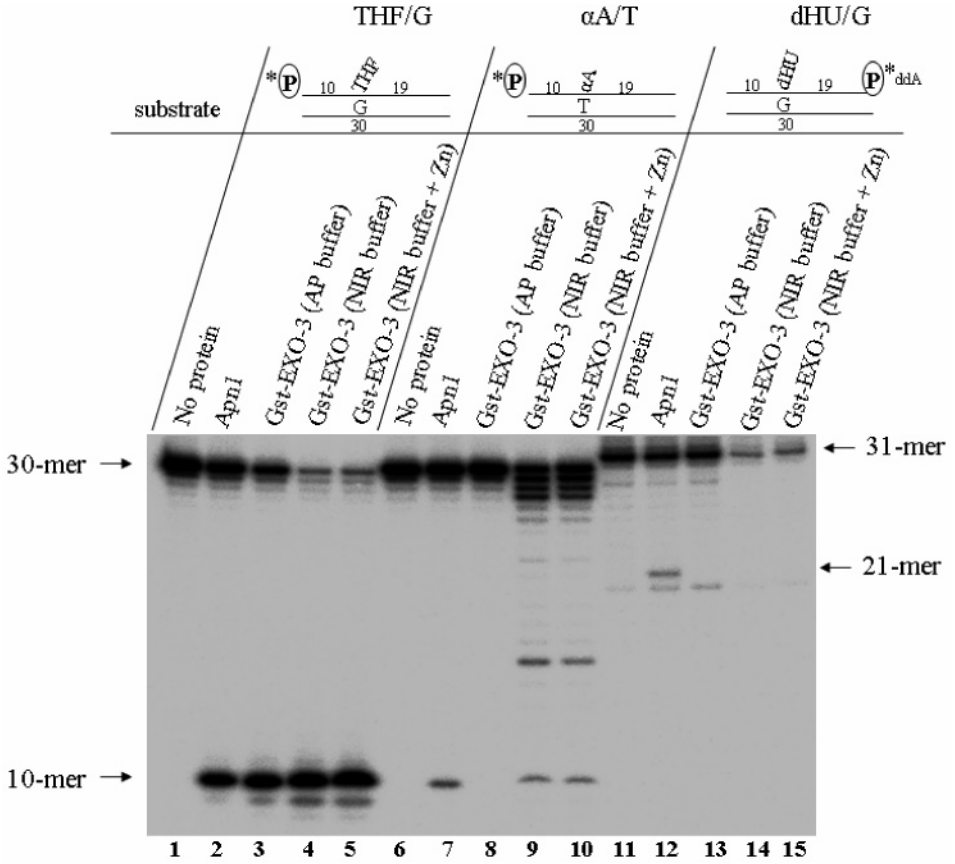

FIGURE 4: Substrate specificity of Gst-EXO-3 under varying buffer conditions. The standard assay mixture for damage-specific activity contained 0.1 pmol of the 5′-[^{32}P] or 3′-[^{32}P]dCMP-end-labeled 30-mer double-stranded oligonucleotide, either THF·G, αdA·T, or dHU·G base pairs, and purified Gst-EXO-3 followed by incubation at 37 °C for 30 min in buffer AP (100 mM Tris/HCl at pH 7.0 and 5 mM $MgCl_2$), buffer NIR (20 mM Hepes-KOH at pH 6.8, 50 mM KCl, 1 mM DTT, 100 μg/mL bovine serum albumin, and 0.5 mM $MgCl_2$), or buffer NIR with Zn (buffer NIR plus 0.1 mM $ZnCl_2$ instead of $MgCl_2$) in a final volume of 20 μL. Lanes 1−5, 5′-end-labeled THF·G substrate; lanes 6−10, 5′-end-labeled αdA·T substrate; and lanes 11−15, 3′-end labeled dHU·G substrate. Lanes 2, 7, and 12 contained 1 ng of purified Apn1; lanes 3−5, 8−10, and 13−15 each contained 145 ng of purified Gst-EXO-3. Reaction products were analyzed by electrophoresis in denaturing 20% (w/v) polyacrylamide−7 M urea gels and visualized by PhosphorImager Storm (Molecular Dynamics, Sunnyvale, CA). The results are representative of two independent analyses.

(4 mM) present in the enzyme storage buffer, which was present in the assay reaction at a final concentration of 0.4 mM. Thus, to assess the importance of divalent metal ions on Gst-EXO-3 enzymatic activities, the assays were performed in the presence of the metal ion chelator EDTA. The AP endonuclease activity of Gst-EXO-3 was completely abolished in the presence of 5 mM EDTA (Figure 5A, lane 11), indicating that the protein requires a divalent metal ion such as Mg^{2+} for the AP endonuclease activity.

The 3′-diesterase activity of Gst-EXO-3 was not evident in the presence of low $MgCl_2$ (0.4 mM) (Figure 5B, lane 1), as observed for the AP endonuclease activity (Figure 5A, lane 1), indicating that this activity has a more stringent requirement for Mg^{2+}. Addition of 5 mM $MgCl_2$ to the assay mixture stimulated the AP endonuclease, as well as revealed the 3′-diesterase activities of Gst-EXO-3 (parts A and B of Figure 5, lane 2, respectively). In independent experiments, neither of these activities was further stimulated by supplementing the reaction mixture with as much as 10 or 15 mM $MgCl_2$ (data not shown). It is noteworthy that higher concentrations of $MgCl_2$ (50 mM) inhibited the AP endonuclease and 3′-diesterase activities (data not shown).

Additional tests were also conducted to determine if the metal ion dependence of the AP endonuclease and 3′-diesterase activities of Gst-EXO-3 was specific for Mg^{2+}. $CaCl_2$ (5 mM) and $MnCl_2$ (5 mM) were each capable of substituting for $MgCl_2$ (parts A and B of Figure 5, lanes 3 and 4). In contrast, $ZnCl_2$ (5 mM) completely inhibited the Mg^{2+}-stimulated AP endonuclease and 3′-diesterase activities (parts A and B of Figure 5, lanes 5 and 6, respectively). The monovalent cations Na^+, Li^+, and K^+ each at 5 mM neither stimulated nor inhibited the AP endonuclease activity and did not stimulate the 3′-diesterase activity of the protein (parts A and B of Figure 5, compare lane 1 with lanes 7−9, respectively).

AP Endonuclease and 3′-Diesterase Activities of the Variant E68A Exhibit Slightly Altered Mg^{2+} Requirements. We were prompted to examine if the Mg^{2+} requirement of E68A is altered with respect to the native Gst-EXO-3 for two reasons: (i) E68A has a reduced level of 3′-diesterase, an activity with a stringent requirement for Mg^{2+}; and (ii) the corresponding amino acid (Glu96) of hApe1 is shown to bind Mg^{2+} and play a critical role in the enzyme catalytic function (*22*). To carry out this experiment, we dialyzed both the purified Gst-EXO-3 and Gst-E68A against the storage buffer lacking $MgCl_2$ followed by the analysis for AP endonuclease and 3′-diesterase activities. As shown in Figure 6A, under this condition, the purified Gst-EXO-3 retained a significant level of AP endonuclease activity (lane 2), which was stimulated by the addition of 1 mM $MgCl_2$ (lane 7). In

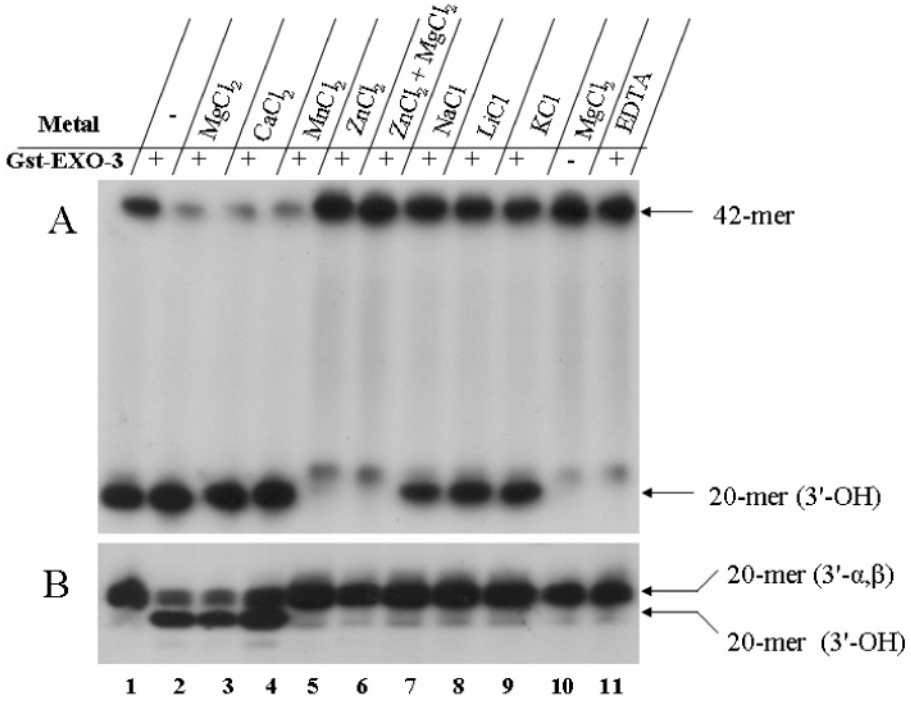

FIGURE 5: Metal ion dependence of Gst-EXO-3 on the processing of AP site and 3′-α,*β* unsaturated aldehyde DNA substrates. (A and B) Purified Gst-EXO-3 (92 ng) was assayed as in Figure 2 in 100 mM Tris-HCl at pH 7.0 but with 0.3 mM $MgCl_2$ (from the enzyme storage buffer) in the presence of the divalent and monovalent ions in the form of the indicated salts to a final concentration of 5 mM. The metal ion chelator (EDTA) was used at 5 mM. Product formation was monitored as in Figure 2 (B and C). The data are representative of three experiments from two independent protein purifications.

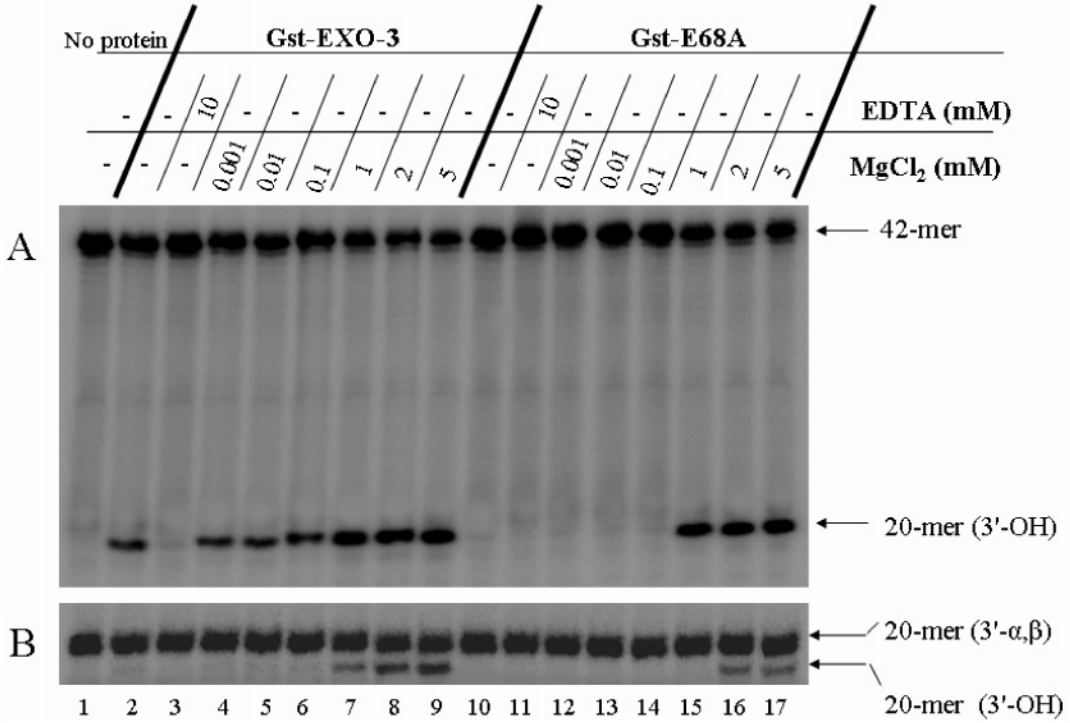

FIGURE 6: Comparison of the Mg^{2+} requirement of Gst-EXO-3 and its variant E68A on incision of damaged DNA substrates. (A and B) Purified Gst-EXO-3 and Gst-E68A were dialyzed twice against storage buffer without $MgCl_2$ and assayed (187 ng) as in Figure 2 in 100 mM Tris-HCl at pH 7.0 with the indicated concentrations of $MgCl_2$ (lanes 4−9 and 12−17) or 10 mM EDTA (lanes 3 and 11). Product formation was monitored as in Figure 2 (B and C).

contrast, the dialyzed Gst-E68A variant showed no detectable AP endonuclease activity (lane 10), unless $MgCl_2$ (1 mM) was added to the reaction (lane 15). In the case of the 3′-diesterase activity, neither dialyzed Gst-EXO-3 nor Gst-E68A was active on the 3′-α,*β* unsaturated aldehyde substrate (Figure 6B, lanes 2 and 10, respectively), except upon the addition of 1 mM $MgCl_2$ for the native protein or 2 mM $MgCl_2$ for the E68A variant protein (Figure 6B, lanes 7 and 16, respectively). These data are consistent with the notion that Mg^{2+} is tightly associated with the native Gst-EXO-3 but not with the variant Gst-E68A. Moreover, it would appear that the Gst-E68A variant displays only a subtle difference

in the Mg^{2+} requirement when compared with the native Gst-EXO-3 protein.

Gst-E68A and not Gst-EXO-3 or D190A Forms a Stable Complex with an AP Site Substrate in the Presence of Crude Extract. Because E68A exhibits AP endonuclease activity *in vitro* in the presence of Mg^{2+}, yet it is unable to confer MMS resistance to strain YW778, raised the possibility that this variant could have a defect beyond the incision step *in vivo*. We therefore tested if E68A binding to the AP-site substrate could be altered. To assess this, we performed a gel mobility-shift assay with crude extracts using the 42-mer double-stranded oligonucleotide AP-site substrate as a probe. Crude extracts derived from either the parent or strain YW778 formed at least two AP endonuclease-independent DNA−protein complexes (designated C3 and C4 for non-relevant complexes) (Figure 7A, lanes 3−7). Extracts derived from strain YW778 expressing the native Gst-EXO-3 did not form any additional DNA−protein complexes (Figure 7A, lane 5), suggesting that under these conditions Gst-EXO-3 is not associated with the AP-site substrate. Interestingly, crude extract derived from strain YW778 expressing Gst-E68A formed a distinct DNA−protein complex (C1), suggesting that this variant harbors a defect causing it to remain bound to the DNA substrate (Figure 7A, lane 6 versus 5). Because the complex C1 migrated much slower than the DNA−protein complex (C2) formed with a control protein, i.e., purified Gst-Apn1 (66 kDa), which is slightly larger than the Gst-E68A (62 kDa) (Figure 7A, lane 6 versus 2), it is possible that the former complex may exhibit an altered structure or arise as a result of association with at least another protein in the extract (see the Discussion). We note that the C1 complex cannot be the result of the Gst portion nonspecifically interacting with a DNA-binding protein, because this complex was not observed with extracts expressing Gst-EXO-3 (Figure 7A, lane 5) or a control fusion protein Gst-Tsa1 (data not shown).

Purified Gst-E68A alone did not form the DNA−protein complex (C1) with the AP-site substrate (Figure 7A, lane 9) but instead required crude extract (Figure 7A, lane 12). Importantly, increasing amounts of purified Gst-E68A showed a concentration-dependent formation of the C1 complex in the presence of crude extract from strain YW778 (Figure 7B, lanes 5−7). In control experiments, where the DNA substrate used was a 42-mer double-stranded oligonucleotide without an AP site (i.e., containing the normal C·G base pair), formation of the C1 complex was only very weakly detected (data not shown), suggesting that the C1 complex formation occurs predominantly with the intact AP-site substrate or its cleaved form. To test this further, we used the same 42-mer double-stranded oligonucleotide substrate but carrying a single U·G mismatch in place of the AP site and examined for C1 complex formation. As shown in Figure 7C (lane 1), purified Gst-E68A in the presence of crude extract derived from strain YW778 was capable of forming the C1 complex with the U·G mismatch DNA. However, formation of this C1 complex was almost completely abolished by the addition of increasing concentrations of Ugi, which specifically inhibits the Ung present in the crude extract (Figure 7C, lanes 2−7). Because crude extract derived from strain YW778 contains Ung activity proficient at removing uracil from the U·G mismatch to create the AP site for Gst-EXO-3 action (Figure 2A, lane 5 versus 6), it is therefore likely that E68A-induced formation of the C1 complex involves an AP site.

Gst-E68A Forms a Stable Complex with 3′-α,β Unsaturated Aldehyde in the Presence of Crude Extract. Because YW778 extract contains several β lyases that can cleave the AP-site substrate, it is possible that the C1 complex may be the result of Gst-E68A associated with 3′-α,β unsaturated aldehyde due to a poor 3′-diesterase activity. To test this possibility, the AP-site substrate was pretreated with endonuclease III to generate the 3′-α,β unsaturated aldehyde, which was used as a probe to monitor for the formation of the C1 complex with purified Gst-E68A. No C1 complex was formed with the 3′-α,β unsaturated aldehyde substrate and purified Gst-E68A (Figure 7D, lane 5), excluding the possibility that Gst-E68A alone can form the C1 complex with this lesion. As observed with the AP-site probe, the C1 complex was formed if crude extract from strain YW778 was added to the reaction mixture containing purified Gst-E68A and the 3′-α,β unsaturated aldehyde substrate (Figure 7D, lane 6). This finding might support the notion that repair of AP-site lesions and single-strand breaks with 3′-blocking groups could involve the association of EXO-3 with at least one other protein *in vivo* and that the E68A variant has a defect that causes it to remain bound to both AP sites and 3′-α,β unsaturated aldehydes.

E68A Forms a DNA−Protein Complex with Extracts Derived from C. elegans Embryos. To assess whether the E68A-induced DNA−protein complex (C1) might be physiologically relevant, the DNA-binding assay with the AP-site substrate was conducted with crude protein extract derived from purified *C. elegans* embryos (*29*). In the absence of Gst-E68A, the *C. elegans* embryonic extract did not form the slow migrating complex (C1) with the AP-site substrate (Figure 8, lane 6). However, addition of purified Gst-E68A to the *C. elegans* embryonic extract induced the formation of the same C1 complex, as with yeast crude extract (Figure 8, lane 7 versus 5). Likewise, crude extracts derived from either *E. coli* or human cells also produced the same slow migrating C1 complex (data not shown), suggesting that there might be a common factor triggering formation of the Gst-E68A DNA−protein complex.

Because human Ape1 interacts with DNA glycosylases to provoke their dissociation from AP sites, we tested whether the factor triggering formation of the C1 complex could be the result of Ung (*38*, *39*). To do this, we used extracts prepared from a yeast parent strain PY32 and the isogenic uracil DNA glycosylase-deficient mutant (*ung*Δ) to assess for the formation of the C1 complex. Addition of purified Gst-E68A to either of these extracts induced equally the formation of the C1 complex (Figure 8, lanes 10 and 11), thus excluding the possibility that uracil DNA glycosylase might be the factor involved in the formation of the Gst-E68A DNA−protein complex.

DISCUSSION

In this study, we used a yeast DNA-repair-deficient mutant devoid of AP endonuclease/3′-diesterase activities to express the *C. elegans* EXO-3 as a functionally active Gst-fusion protein. This Gst-EXO-3 protein was affinity-purified and characterized for its enzymatic activities. We show that the purified Gst-EXO-3 possesses both AP endonuclease and 3′-

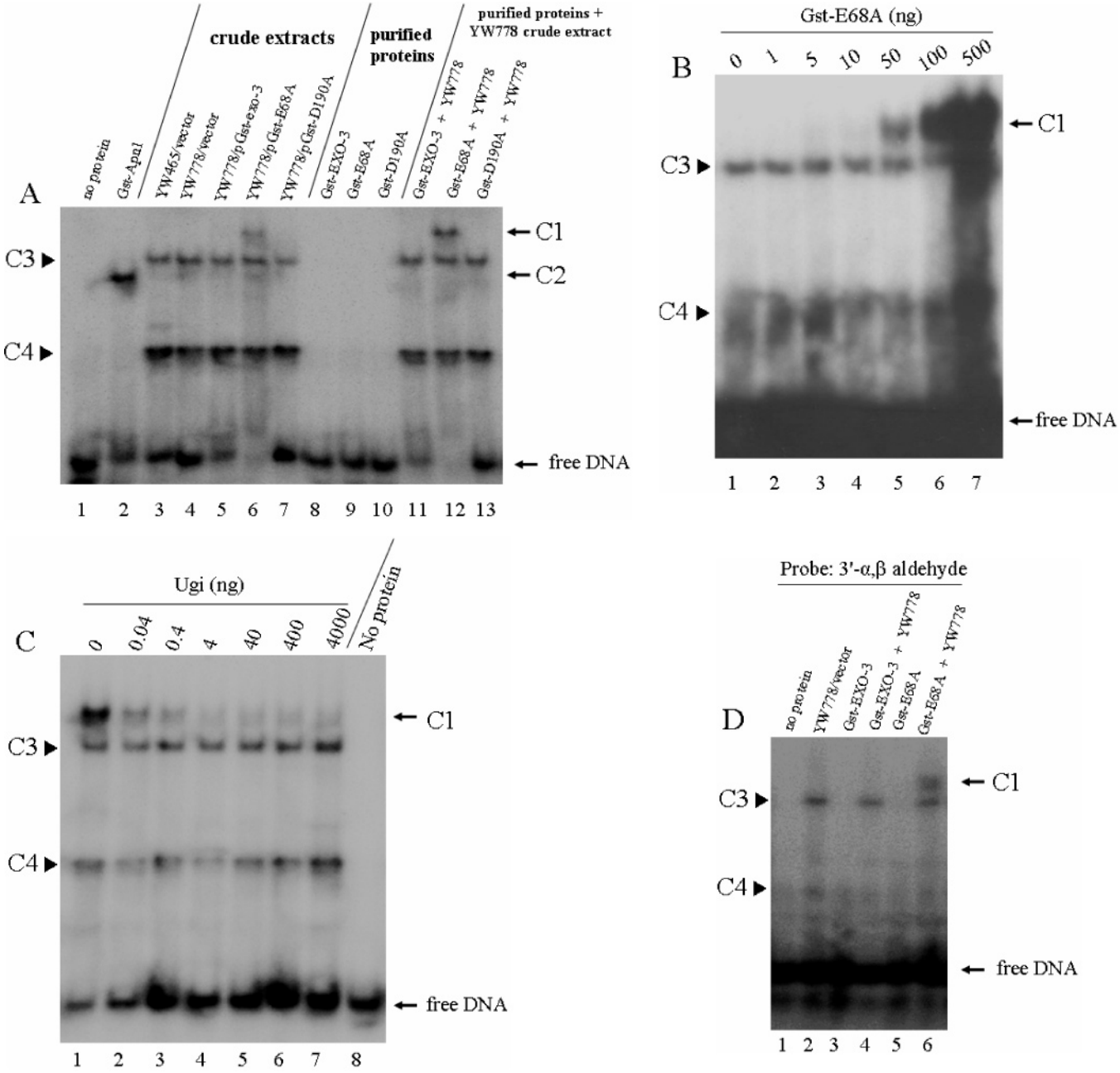

FIGURE 7: Mobility-shift analyses of lesion containing oligonucleotide substrates by native Gst-EXO-3 and the variants Gst-E68A and Gst-D190A. The samples were incubated with 0.5 ng of 5′-^{32}P-labeled 42-mer double-stranded oligonucleotide in DNA-binding buffer (see the Materials and Methods). (A) Mobility-shift assay with the AP-site probe in the presence of either 10 μg of crude protein extract derived from the parent YW465 or the mutant strain YW778 carrying the indicated vector or plasmids (lanes 3−7), 100 ng of affinity-purified protein (lanes 8−10), or a combination of crude extract (10 μg) derived from strain YW778 plus 100 ng of purified protein (lanes 11−13) at 25 °C for 20 min. Controls: no protein (lane 1) and 100 ng of purified Gst-Apn1 (lane 2). (B) Binding of increasing amounts of purified Gst-E68A to the AP-site probe in the presence of a fixed concentration of crude extract (10 μg) derived from strain YW778. Lane 1, crude extract without purified Gst-E68A; lanes 2−7, crude extract with 1−500 ng of purified Gst-E68A, respectively. (C) Preference of the substrate with an AP site for DNA binding of Gst-E68A. The substrate uracil·guanine (U·G) mismatch was incubated with 10 μg of crude extract derived from strain YW778 containing endogenous uracil DNA glycosylase and 100 ng of purified Gst-E68A in the absence of uracil glycosylase inhibitor Ugi (lane 1) or in the presence of increasing concentrations (0.04−4000 ng) of Ugi (lanes 2−7) to inhibit formation of AP sites. (D) Mobility-shift assay with the 3′-α,β unsaturated aldehyde probe in the presence of either crude protein extract derived from strain YW778 or purified Gst-fusion protein. Lane 1, probe alone; lane 2, 10 μg of crude extract from strain YW778 carrying the vector; lane 3, 100 ng of purified Gst-EXO-3; lane 4, a combination of Gst-EXO-3 and crude extract; lane 5, 100 ng of purified Gst-E68A; and lane 6, a combination of purified Gst-E68A and crude extract. Formation of the protein−DNA complexes were resolved on 6% native polyacrylamide (39:1 acrylamide/bis-acrylamide) gels by electrophoresis in a high ionic strength Tris-glycine buffer and revealed by autoradiography. C1 and C2, specific complexes formed in the presence of purified Gst-E68A and Gst-Apn1, respectively. C3 and C4, nonrelevant complexes.

diesterase activities and that a variant D190A completely lacks these activities. These findings are consistent with the identity that exists between *C. elegans* EXO-3 and the well-defined exo III family members, e.g., *E. coli* exonuclease III and human Ape1, and further indicate that EXO-3 may indeed perform a biologically conserved role in DNA repair (*29*). As such, we anticipate that *C. elegans* mutants deficient in EXO-3 function will exhibit hypersensitivity to DNA-

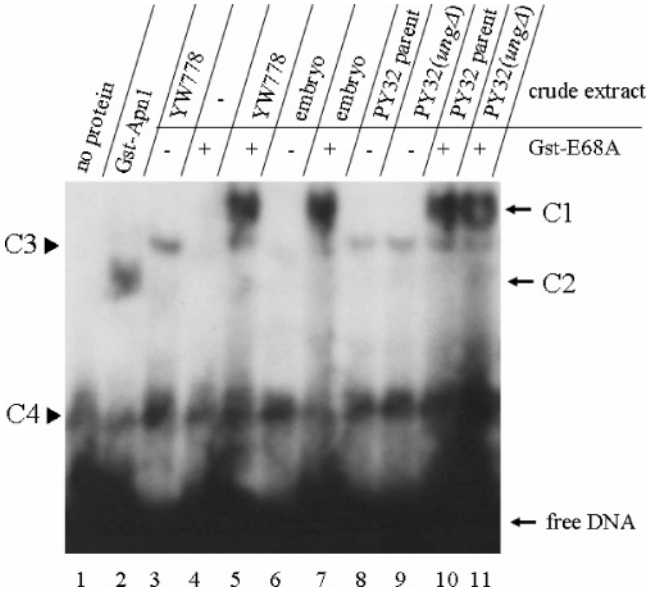

FIGURE 8: Mobility-shift analysis of the AP-site substrate in the presence of crude extract derived from either yeast cells or *C. elegans* embryos. Crude protein extracts (10 μg) derived from either the indicated yeast strains YW778, PY32 (parent), or PY32 (*ung*Δ deleted for the gene encoding uracil DNA glycosylase) or purified embryos from *C. elegans* that were incubated without (lanes 3, 6, 8, and 9) or with (lanes 4, 5,7, 10, and 11) 100 ng of purified Gst-E68A. Controls: no protein (lane 1) and 100 ng of Gst-Apn1 (lane 2). Complex formation was monitored as in Figure 7. C1 and C2, specific complexes formed in the presence of purified Gst-E68A and Gst-Apn1, respectively. C3 and C4, nonrelevant complexes.

damaging agents that create AP sites and strand breaks with blocked 3′ ends. Moreover, these *C. elegans* mutants are expected to display genetic instability, unless the functional role of EXO-3 can be fully compensated by the second AP endonuclease/3′-diesterase APN-1 that also exists in this organism.

Members of the exo III family display varying levels of AP endonuclease and 3′-diesterase activities. For example, the AP endonuclease and 3′-diesterase activities of *E. coli* exonuclease III are nearly equal (*40*, *41*). However, the AP endonuclease activity of the human Ape1 is substantially higher than its 3′-diesterase activity; the k_{cat} for AP-site cleavage is 70−400-fold greater than that for the removal of 3′-phosphoglycolate (*42*). In this respect, we believe that *C. elegans* EXO-3, which has equally strong AP endonuclease and 3′-diesterase activity, is more similar to *E. coli* exonuclease III. At the moment, it is difficult to compare the activities of the *C. elegans* EXO-3 enzyme with the AP endonuclease/3′-diesterase activities from other organisms. Several factors could limit this comparison, for example, we cannot quantitatively assess what fraction of the Gst-EXO-3 purified from yeast is inactive because of improper folding as a consequence of being in a different milieu. Moreover, we have not further purified the Gst-EXO-3 to eliminate possible minor contaminating proteins that could interfere with the enzyme activities. Nonetheless, we believe that the Gst fragment does not interfere with EXO-3 enzymatic functions, because other tagged proteins, e.g., Gst-Apn1 and Gst-hApe1, retain full function. In fact, Gst-EXO-3 can fully substitute for both the yeast Apn1 and Apn2 in the repair of spontaneous and drug-induced DNA damage (*20*).

We have not observed a strong 3′ → 5′ exonuclease activity following cleavage of the AP site by the Gst-EXO-3, as we previously demonstrated for *E. coli* exonuclease III (*28*), suggesting that the enzyme either lacks such major exonuclease activity or is unable to process the nicked AP site. In fact, yeast Apn1 shows minimal 3′ → 5′ exonucleolytic activity following cleavage of AP sites (*6*). Recently, we have shown that Apn1 contains a potent 3′ → 5′ exonuclease activity toward recessed DNA duplexes, which strongly depends upon the ionic strength and sequence context (*43*). In our experiments, we have not explored the ability of Gst-EXO-3 to process recessed DNA substrates, but we note that this enzyme has a powerful exonuclease activity on blunt-ended DNA substrates, even in the presence of DNA lesions, e.g., αA and dHU (Figure 4, lanes 9−10 and 14−15, respectively). This activity is not the result of a contaminating yeast exonuclease, because similar processing of the blunt-ended DNA substrate was observed with the purified Gst-EXO-3 and crude extract derived from strain YW778 expressing Gst-EXO-3 but not with the strain carrying the empty vector (data not shown). The purpose of this powerful 3′ → 5′ exonuclease activity toward fully duplex DNA remains to be explored, although it could play a role in processing the ends of DNA double-strand breaks to stimulate nonhomologous DNA end joining. In fact, we have observed that Gst-EXO-3 can confer more than parental resistance to strain YW778 following challenges with bleomycin, an antitumor drug that can create DNA double-strand breaks, as well as AP sites and DNA-strand breaks with blocked 3′ ends (*20*, *44*).

The Mg^{2+} dependence of members of the exonuclease III family of hydrolytic AP endonucleases has been established in *E. coli* and humans (*45*−*47*). Herein, we show that both the AP endonuclease and 3′-diesterase activities of *C. elegans* EXO-3 are dependent upon divalent metal ions such as Mg^{2+}, Ca^{2+}, and Mn^{2+}. However, the two enzymatic activities exhibit different requirements for metal ions. We show that the AP endonuclease activity is functionally active even in extracts that have been dialyzed to remove any unbound Mg^{2+}, whereas the 3′-diesterase activity requires the addition of at least 1 mM Mg^{2+} in addition to any Mg^{2+} bound to the protein. This difference in the Mg^{2+} requirement does not appear to create a differential effect on the ability of EXO-3 to process damaged DNA *in vivo*, because Gst-EXO-3 can fully restore to the AP endonuclease/3′-diesterase-deficient strain resistance to various DNA-damaging agents that are known to create AP sites and single-strand breaks with blocked 3′ ends (Figure 1C) (*20*). It is believed that Mg^{2+} aids these DNA-repair enzymes by playing a role in coordinating DNA binding and in catalyzing DNA cleavage (*30*, *47*). The human Ape1 had been originally thought to have only one metal-ion-binding site, coordinated by the amino acid residues D70 and E96 (*48*). Elucidation of the crystal structure of hApe1 at different pH values has shown that, at pH 7.5, there is a second metal-binding site in the active site of the protein, at a distance of about 5 Å from the first, which is coordinated by H309, D210, and N212 (*49*). The fact that the amino acids involved in both binding sites are conserved in the *C. elegans* EXO-3 protein, suggests that this enzyme may also contain two Mg^{2+}-binding sites. At the moment, we do not know whether the second potential Mg^{2+}-binding site plays a role in EXO-3 catalytic and/or DNA-binding activity. However, it is noteworthy that AP endonuclease activity was observed at concentrations of

Mg^{2+} that were too low for the 3′-diesterase activity, raising the possibility that more than one metal-binding site might be required for optimal 3′-diesterase activity.

Crystal structure analysis revealed that Glu34 of *E. coli* exonuclease III, which corresponds to Glu68 of *C. elegans* EXO-3, is a divalent metal-ion-binding site (*22*). Previous genetic studies with the human Ape1 protein suggested that the Glu96 residue, which corresponds to Glu68 of *C. elegans* EXO-3, provides the critical metal-binding side chain required for catalysis and is involved in establishing the precise active-site chemistry of the enzyme (*22*, *50*). Substitution of Glu96 for alanine in human Ape1 resulted in a variant with a drastically reduced (∼225-fold) ability to cleave AP sites as compared to the native hApe1, even in the presence of 5 mM Mg^{2+} (*22*). However, unlike the hApe1 variant E96A, the EXO-3 variant E68A showed a significant level of AP endonuclease activity in the presence of 5 mM Mg^{2+} but which was undetectable if the Mg^{2+} concentration was lower than 1 mM (Figure 6). This latter observation is consistent with the notion that Glu68 of EXO-3 is required to coordinate Mg^{2+} for the enzyme catalytic mechanism (*48*). The precise role of Mg^{2+} cannot be determined from these studies, but it could play a role in the enzyme active site to facilitate catalytic cleavage of the sugar phosphate bond and/or to trigger disassociation of the enzyme following cleavage of the damaged DNA.

The observation that the E68A variant forms a distinct and stable complex with the AP-site lesion in the presence of crude extracts derived from either yeast or the embryos of *C. elegans* suggests that there might be a factor associated with EXO-3 during the repair of AP-site lesions. In fact, a DNA−protein complex of the same size is also formed following incubation of the purified E68A and the AP-site substrate with either *E. coli* or human cell extracts (data not shown), suggesting that this factor could serve a common role in the repair of AP-site lesions in other organisms. One possible function of this factor might be to aid in the recognition of AP sites and/or to recruit EXO-3 to the lesion. After incision, the protein complex may undergo a structural change to permit disassociation from the DNA. However, E68A together with the protein factor may be unable to undergo this conformational change and as a result remain associated with the incised DNA. It is noteworthy that we have not directly tested whether the C1 complex indeed consists of an incised AP-site substrate, although conditions that are conducive to AP-site nicking by Gst-E68A such as addition of Mg^{2+} (5 mM) to the crude extract did not significantly disrupt the formation of the C1 complex (data not shown). As such, the C1 complex could represent Gst-E68A associated with nicked AP-site DNA. This is a reasonable possibility because Gst-E68A added to crude extract also generated the C1 complex when the AP-site substrate is precleaved by the β lyase endonuclease III.

Formation of the C1 complex could also be explained if E68A independently recognizes the AP site but is unable to rapidly disassociate from the incised DNA, as well as from other substrate DNA lesions terminated with 3′-blocking groups such as 3′-α,β unsaturated aldehyde. As such, E68A may remain bound to the DNA when subsequent components of the base-excision repair machinery, e.g., DNA polymerase, assemble onto the DNA (*51*). If so, this might explain the lack of detecting a DNA−protein complex with only the purified Gst-E68A variant and either the AP-site or 3′-α,β unsaturated aldehyde substrate. In this case, the inability of Gst-E68A to disassociate from the lesion might result in a stalled complex that hinders the base-excision repair process. While our data supports the notion that a candidate protein may be associated with the C1 complex, we cannot exclude the possibility that a nonprotein cofactor or even a nonspecific protein in the crude extracts may trigger a conformational change of Gst-E68A bound to the AP-site or 3′-α,β unsaturated aldehyde substrate, thus, causing the complex to migrate very slowly. Nonetheless, we believe that characterization of this C1 complex may shed some light on the function of the Glu68 residue of EXO-3 as well as identify other possible players of the base-excision repair pathway.

ACKNOWLEDGMENT

We gratefully acknowledge Dr. Bob Melamede and the late Dr. Dale Mosbaugh for providing us with the endo III and Ugi proteins and Dr. Tom Wilson for the yeast strains. We also thank Dr. Tadahide Izumi and Ms. Ratsavarinh Vongsamphanh for critically reading the manuscript, Xiaoming Yang for purified endo IV and Gst-Apn1, and Anick Leduc for help with the site-directed mutagenesis.

REFERENCES

1. Cunningham, R. P. (1997) DNA glycosylases, *Mutat. Res. 383*, 189−196.
2. Krokan, H. E., Standal, R., and Slupphaug, G. (1997) DNA glycosylases in the base excision repair of DNA, *Biochem. J. 325*, 1−16.
3. Lindahl, T., and Nyberg, B. (1972) Rate of depurination of native deoxyribonucleic acid, *Biochemistry 11*, 3610−3618.
4. Demple, B., and Harrison, L. (1994) Repair of oxidative damage to DNA: Enzymology and biology, *Annu. Rev. Biochem. 63*, 915−948.
5. Ramotar, D. (1997) The apurinic−apyrimidinic endonuclease IV family of DNA repair enzymes, *Biochem. Cell Biol. 75*, 327−336.
6. Vance, J. R., and Wilson, T. E. (2001) Repair of DNA strand breaks by the overlapping functions of lesion-specific and non-lesion-specific DNA 3′ phosphatases, *Mol. Cell Biol. 21*, 7191−7198.
7. Kerins, S. M., Collins, R., and McCarthy, T. V. (2003) Characterization of an endonuclease IV 3′ → 5′ exonuclease activity, *J. Biol. Chem. 278*, 3048−3054.
8. Jilani, A., Vongsamphanh, R., Leduc, A., Gros, L., Saparbaev, M., and Ramotar, D. (2003) Characterization of two independent amino acid substitutions that disrupt the DNA repair functions of the yeast Apn1, *Biochemistry 42*, 6436−6445.
9. Wilson, D. M., III, Takeshita, M., Grollman, A. P., and Demple, B. (1995) Incision activity of human apurinic endonuclease (Ape) at abasic site analogs in DNA, *J. Biol. Chem. 270*, 16002−16007.
10. Chou, K. M., and Cheng, Y. C. (2003) The exonuclease activity of human apurinic/apyrimidinic endonuclease (APE1). Biochemical properties and inhibition by the natural dinucleotide Gp4G, *J. Biol. Chem. 278*, 18289−18296.
11. Barzilay, G., and Hickson, I. D. (1995) Structure and function of apurinic/apyrimidinic endonucleases, *Bioessays 17*, 713−719.
12. Chan, E., and Weiss, B. (1987) Endonuclease IV of *Escherichia coli* is induced by paraquat, *Proc. Natl. Acad. Sci. U.S.A. 84*, 3189−3193.
13. Johnson, A. W., and Demple, B. (1988) Yeast DNA diesterase for 3′-fragments of deoxyribose: Purification and physical properties of a repair enzyme for oxidative DNA damage, *J. Biol. Chem. 263*, 18009−18016.
14. Popoff, S. C., Spira, A. I., Johnson, A. W., and Demple, B. (1990) Yeast structural gene (APN1) for the major apurinic endonuclease: Homology to *Escherichia coli* endonuclease IV, *Proc. Natl. Acad. Sci. U.S.A. 87*, 4193−4197.

15. Johnson, R. E., Torres-Ramos, C. A., Izumi, T., Mitra, S., Prakash, S., and Prakash, L. (1998) Identification of APN2, the *Saccharomyces cerevisiae* homolog of the major human AP endonuclease HAP1, and its role in the repair of abasic sites [in process citation], *Genes Dev. 12*, 3137−3143.
16. Bennett, R. A. (1999) The *Saccharomyces cerevisiae* ETH1 gene, an inducible homolog of exonuclease III that provides resistance to DNA-damaging agents and limits spontaneous mutagenesis, *Mol. Cell Biol. 19*, 1800−1809.
17. Demple, B., Herman, T., and Chen, D. S. (1991) Cloning and expression of APE, the cDNA encoding the major human apurinic endonuclease: Definition of a family of DNA repair enzymes, *Proc. Natl. Acad. Sci. U.S.A. 88*, 11450−11454.
18. Hadi, M. Z., and Wilson, D. M., III (2000) Second human protein with homology to the *Escherichia coli* abasic endonuclease exonuclease III, *Environ. Mol. Mutagen. 36*, 312−324.
19. Masson, J. Y., Tremblay, S., and Ramotar, D. (1996) The *Caenorhabditis elegans* gene CeAPN1 encodes a homolog of *Escherichia coli* and yeast apurinic/apyrimidinic endonuclease, *Gene 179*, 291−293.
20. Shatilla, A., Leduc, A., Yang, X., and Ramotar, D. (2005) Identification of two apurinic/apyrimidinic endonucleases from *Caenorhabditis elegans* by cross-species complementation, *DNA Repair 4*, 655−670.
21. Barzilay, G., Walker, L. J., Robson, C. N., and Hickson, I. D. (1995) Site-directed mutagenesis of the human DNA repair enzyme HAP1: Identification of residues important for AP endonuclease and RNase H activity, *Nucleic Acids Res. 23*, 1544−1550.
22. Barzilay, G., Mol, C. D., Robson, C. N., Walker, L. J., Cunningham, R. P., Tainer, J. A., and Hickson, I. D. (1995) Identification of critical active-site residues in the multifunctional human DNA repair enzyme HAP1, *Nat. Struct. Biol. 2*, 561−568.
23. Yang, X., Tellier, P., Masson, J. Y., Vu, T., and Ramotar, D. (1999) Characterization of amino acid substitutions that severely alter the DNA repair functions of *Escherichia coli* endonuclease IV, *Biochemistry 38*, 3615−3623.
24. Ishchenko, A. A., Sanz, G., Privezentzev, C. V., Maksimenko, A. V., and Saparbaev, M. (2003) Characterisation of new substrate specificities of *Escherichia coli* and *Saccharomyces cerevisiae* AP endonucleases, *Nucleic Acids Res. 31*, 6344−6353.
25. Sambrook, J., Fritsch, E. F., and Maniatis, T. (1989) in *Cold Spring Harbor Laboratory Press*, Cold Spring Harbor, New York.
26. Bradford, M. M. (1976) A rapid and sensitive method for the quantitation of microgram quantities of protein utilizing the principle of protein-dye binding, *Anal. Biochem. 72*, 248−254.
27. Ramotar, D., and Masson, J. Y. (1996) A *Saccharomyces cerevisiae* mutant defines a new locus essential for resistance to the antitumour drug bleomycin, *Can. J. Microbiol. 42*, 835−843.
28. Masson, J. Y., and Ramotar, D. (1997) Normal processing of AP sites in Apn1-deficient *Saccharomyces cerevisiae* is restored by *Escherichia coli* genes expressing either exonuclease III or endonuclease III, *Mol. Microbiol. 24*, 711−721.
29. Shatilla, A., and Ramotar, D. (2002) Embryonic extracts derived from the nematode *Caenorhabditis elegans* remove uracil from DNA by the sequential action of uracil-DNA glycosylase and AP (apurinic/apyrimidinic) endonuclease, *Biochem. J. 365*, 547−553.
30. Gros, L., Ishchenko, A. A., Ide, H., Elder, R. H., and Saparbaev, M. K. (2004) The major human AP endonuclease (Ape1) is involved in the nucleotide incision repair pathway, *Nucleic Acids Res. 32*, 73−81.
31. Swanson, R. L., Morey, N. J., Doetsch, P. W., and Jinks-Robertson, S. (1999) Overlapping specificities of base excision repair, nucleotide excision repair, recombination, and translesion synthesis pathways for DNA base damage in *Saccharomyces cerevisiae*, *Mol. Cell Biol. 19*, 2929−2935.
32. van der Kemp, P. A., Thomas, D., Barbey, R., de Oliveira, R., and Boiteux, S. (1996) Cloning and expression in *Escherichia coli* of the OGG1 gene of *Saccharomyces cerevisiae*, which codes for a DNA glycosylase that excises 7,8-dihydro-8-oxoguanine and 2,6-diamino-4-hydroxy-5-*N*-methylformamidopyrimidine, *Proc. Natl. Acad. Sci. U.S.A. 93*, 5197−5202.
33. Meadows, K. L., Song, B., and Doetsch, P. W. (2003) Characterization of AP lyase activities of *Saccharomyces cerevisiae* Ntg1p and Ntg2p: Implications for biological function, *Nucleic Acids Res. 31*, 5560−5567.
34. Girard, P. M., Guibourt, N., and Boiteux, S. (1997) The Ogg1 protein of *Saccharomyces cerevisiae*: A 7,8-dihydro-8- oxoguanine DNA glycosylase/AP lyase whose lysine 241 is a critical residue for catalytic activity, *Nucleic Acids Res. 25*, 3204−3211.
35. Johnson, A. W., and Demple, B. (1988) Yeast DNA 3′-repair diesterase is the major cellular apurinic/apyrimidinic endonuclease: Substrate specificity and kinetics, *J. Biol. Chem. 263*, 18017−18022.
36. Unk, I., Haracska, L., Prakash, S., and Prakash, L. (2001) 3′-Phosphodiesterase and 3′ → 5′ exonuclease activities of yeast Apn2 protein and requirement of these activities for repair of oxidative DNA damage, *Mol. Cell Biol. 21*, 1656−1661.
37. Demple, B., Johnson, A., and Fung, D. (1986) Exonuclease III and endonuclease IV remove 3′ blocks from DNA synthesis primers in H_2O_2-damaged *Escherichia coli*, *Proc. Natl. Acad. Sci. U.S.A. 83*, 7731−7735.
38. Waters, T. R., Gallinari, P., Jiricny, J., and Swann, P. F. (1999) Human thymine DNA glycosylase binds to apurinic sites in DNA but is displaced by human apurinic endonuclease 1, *J. Biol. Chem. 274*, 67−74.
39. Marenstein, D. R., Chan, M. K., Altamirano, A., Basu, A. K., Boorstein, R. J., Cunningham, R. P., and Teebor, G. W. (2003) Substrate specificity of human endonuclease III (hNTH1). Effect of human APE1 on hNTH1 activity, *J. Biol. Chem. 278*, 9005−9012.
40. Siwek, B., Bricteux-Gregoire, S., Bailly, V., and Verly, W. G. (1988) The relative importance of *Escherichia coli* exonuclease III and endonuclease IV for the hydrolysis of 3′-phosphoglycolate ends in polydeoxynucleotides, *Nucleic Acids Res. 16*, 5031−5038.
41. Bernelot-Moens, C., and Demple, B. (1989) Multiple DNA repair activities for 3′-deoxyribose fragments in *Escherichia coli*, *Nucleic Acids Res. 17*, 587−600.
42. Suh, D., Wilson, D. M., III, and Povirk, L. F. (1997) 3′-Phosphodiesterase activity of human apurinic/apyrimidinic endonuclease at DNA double-strand break ends, *Nucleic Acids Res. 25*, 2495−2500.
43. Ishchenko, A. A., Yang, X., Ramotar, D., and Saparbaev, M. (2005) The 3′ → 5′ exonuclease of Apn1 provides an alternative pathway to repair 7,8-dihydro-8-oxodeoxyguanosine in *Saccharomyces cerevisiae*, *Mol. Cell Biol.*, in press.
44. Ramotar, D., and Wang, H. (2003) Protective mechanisms against the antitumor agent bleomycin: Lessons from *Saccharomyces cerevisiae*, *Curr. Genet. 43*, 213−224.
45. Gossard, F., and Verly, W. G. (1978) Properties of the main endonuclease specific for apurinic sites of *Escherichia coli* (endonuclease VI). Mechanism of apurinic site excision from DNA, *Eur. J. Biochem. 82*, 321−332.
46. Strauss, P. R., Beard, W. A., Patterson, T. A., and Wilson, S. H. (1997) Substrate binding by human apurinic/apyrimidinic endonuclease indicates a Briggs−Haldane mechanism, *J. Biol. Chem. 272*, 1302−1307.
47. Masuda, Y., Bennett, R. A., and Demple, B. (1998) Rapid dissociation of human apurinic endonuclease (Ape1) from incised DNA induced by magnesium, *J. Biol. Chem. 273*, 30360−30365.
48. Mol, C. D., Izumi, T., Mitra, S., and Tainer, J. A. (2000) DNA-bound structures and mutants reveal abasic DNA binding by APE1 and DNA repair coordination [corrected], *Nature 403*, 451−456.
49. Beernink, P. T., Segelke, B. W., Hadi, M. Z., Erzberger, J. P., Wilson, D. M., III, and Rupp, B. (2001) Two divalent metal ions in the active site of a new crystal form of human apurinic/apyrimidinic endonuclease, Ape1: Implications for the catalytic mechanism, *J. Mol. Biol. 307*, 1023−1034.
50. Erzberger, J. P., and Wilson, D. M., III (1999) The role of Mg^{2+} and specific amino acid residues in the catalytic reaction of the major human abasic endonuclease: New insights from EDTA-resistant incision of acyclic abasic site analogs and site-directed mutagenesis, *J. Mol. Biol. 290*, 447−457.
51. Bennett, R. A., Wilson, D. M., III, Wong, D., and Demple, B. (1997) Interaction of human apurinic endonuclease and DNA polymerase β in the base excision repair pathway, *Proc. Natl. Acad. Sci. U.S.A. 94*, 7166−7169.

BI050195T